Journal of Power Sources 193 (2009) 175–179

Contents lists available at ScienceDirect

Journal of Power Sources

journal homepage: www.elsevier.com/locate/jpowsour

Short communication

Electronic conductivity of modified $La_{0.95}Ni_{0.6}Fe_{0.4}O_{3-\delta}$ perovskites

Elena Konysheva*, John T.S. Irvine

School of Chemistry, University of St Andrews, St Andrews, Fife, KY 16 9ST, UK

ARTICLE INFO

Article history:
Received 18 November 2008
Received in revised form 16 December 2008
Accepted 19 December 2008
Available online 7 January 2009

Keywords:
Modified perovskite
Small additives
Semiconducting-metal transition
Neutron powder diffraction

ABSTRACT

Phase composition and electronic conductivity of $La_{0.95}Ni_{0.6}Fe_{0.4}O_{3-\delta}$ (LNF) modified by small additions (2–10 mol%) of MnO_2, TiO_2, CeO_2 and Sr-containing manganese perovskite were investigated. A-site deficiency was found to be only limited in extent with typically NiO precipitates compensating for the nominal A-site deficiency. The phase composition of modified LNF varies depending on the type and amount of oxide additives. A low level of doping (~2 mol%) does not change the value of conductivity and temperature of the semiconducting-metallic transition (~300 °C). However, electronic conductivity of the modified LNF decreases if it contains 5 mol% of oxide additive or more. A decrease in conductivity was observed independently whether a secondary phase is present, solid solutions form or a change in symmetry of the modified LNF occurs. After reduction in argon atmosphere all compositions investigated exhibit semiconducting behaviour in a wide temperature range. Neutron powder diffraction measurements give insight into the mechanism of solid state interaction of LNF with small degrees of oxide additives.

1. Introduction

Perovskite related materials containing 3d transition metals are important as electrodes in high-efficiency power devices. However, incorporation of materials with promising properties in real systems is very often limited by their compatibility with other components (in the case of cathodes, for instance, with interconnect and electrolytes). Chemical compatibility experiments for complex oxides containing transition metals have to be carried out each time because it is difficult to predict final products of solid state interaction and, as consequence, transport properties of multi-component system. Very often data obtained for perovskite materials containing three 3d transition elements can be in contradiction with the tendencies known for ternary systems [1–4]. One of the reasons is that transition elements situated on the B sublattice of the perovskite structure (for instance Mn, Ni and Fe) are able to change oxidation state simultaneously though the "double exchange mechanism" [5] without variation in oxygen stoichiometry.

$LaNi_{1-y}Fe_yO_{3-\delta}$ perovskites are considered as promising materials for application as an electrode and current collector in solid oxide fuel cells (SOFCs) at intermediate temperatures due to their high, metallic-like electrical conductivity and sufficient stability at elevated temperatures [1]. In addition, lanthanum iron nickelate is more tolerant to the presence of chromia compared to perovskite-type oxides based on lanthanum manganites and cobaltites that allows to minimize chromium poisoning effect [6,7]. The $LaNi_{0.6}Fe_{0.4}O_{3-\delta}$ perovskite has the highest electronic conductivity among $LaNi_{1-y}Fe_yO_{3-\delta}$ series. $LaNi_{0.6}Fe_{0.4}O_{3-\delta}$ shows metallic conductivity at a temperature higher than 200 °C [1,3,4]. Temperature of the semiconducting-metallic transition can be essentially affected by a doping. Particularly, it was found for $La_{0.95}Ni_{0.6}Fe_{0.4}O_{3-\delta}$ (LNF) that simultaneous substitution of Sr and Mn for La and Ni/Fe, respectively, into the A and B sublattices gradually increased the temperature of the semiconducting-metallic transition up to about 840 °C [3]. It was assumed that a high occupancy of the sites of the B sublattice of LNF by Ni (50% or more) seems to be an important requirement for the realisation of the metallic-like conductivity in LNF. Note that $LaNi_{0.4}Fe_{0.6}O_{3-\delta}$ composition (with less than 50 mol% Ni occupancy on the B site) exhibits only semiconducting behaviour [2]. Metallic-like behaviour in $La_{0.9}Sr_{0.1}Ga_{1-x}Ni_xO_3$ ($x = 0.1–0.5$) series was also observed only for the composition containing 50 mol% of Ni cations on the B sublattice [8].

Therefore, this investigation aims to the study phase composition and electronic conductivity of the LNF modified by small additions (2–10 mol%) of transition elements oxides (Mn, Ti), CeO_2 as an off-stoichiometric phase, and Sr-containing manganese perovskite. All these additions can be incorporated into LNF at the stage of production of multi-component solid oxide fuel cells (from electrolytes) and during their performance under real conditions (from oxide scale thermally growing on the surface of interconnects or from contact layers) [9–12]. In addition, an effect of oxygen partial pressure on conductivity of modified LNF and temperature of the semiconducting-metallic transition was explored.

Abbreviations: XRD, X-ray powder diffraction; NPD, neutron powder diffraction.

* Corresponding author. Tel.: +44 1334 463844; fax: +44 1334 463808.
E-mail address: ek31@st-andrews.ac.uk (E. Konysheva).

0378-7753/$ – see front matter © 2008 Elsevier B.V. All rights reserved.
doi:10.1016/j.jpowsour.2008.12.117

2. Experimental

2.1. Sample preparation

Initial perovskite composition $La_{0.95}Ni_{0.6}Fe_{0.4}O_{3-\delta}$ was produced by combustion spray pyrolysis and supplied by PRAXAIR Inc., USA. MnO_2 and TiO_2 were delivered by ALFA AESAR (Lancashire, UK). CeO_2 was delivered by ACROS ORGANICS (New Jerse, USA). $La_{0.8}Sr_{0.2}MnO_3$ (LSM) was supplied by PRAXAIR Inc., USA. CeO_2 was calcinated at 1000 °C for 5 h to remove adsorbed water. The following compositions 98LNF·2CeO_2 (LNFC2), 90LNF·10CeO_2 (LNFC10), 98LNF·2TiO_2 (LNFT2), 95LNF·5TiO_2 (LNFT5), 98LNF·2LSM (LNFSM2) and 90LNF·10LSM (LNFSM10) were obtained by mechanical mixing of LNF and relevant oxides, and followed by calcination in air at 1350 °C for 5 h. The initial LNF was also calcined under the same conditions. In addition, LNF powder was reduced under flowing argon at 800 °C for 12 h. This sample was assigned as LNF-red.

2.2. Experimental methods

X-ray powder diffraction (XRD) data were recorded in air at room temperature (RT) in transmission mode on a Stoe Stadi-P diffractometer with $Cu_{K\alpha}$ radiation (Stoe & Cie GmbH, Darmstadt, Germany) and in reflection mode on Philips analytical X-ray PW1710 diffractometer with $Cu_{K\alpha}$ radiation (Nederlandse Philips Bedrijven B.V., Almelo, The Netherlands). Neutron powder diffraction (NPD) measurements were carried out for LNF, LNF-red and LNFM2 at the Institute Laue Langevin (ILL) in Grenoble on D1A instrument, using a wavelength $\lambda = 1.909$ Å. The diffraction spectra were registered in the angular range $0° \leq 2\Theta \leq 158°$, in steps of 0.05° at room temperature. The diffraction data were refined by the Rietveld method [13,14], using the FullProf program [15].

Electrical conductivity was measured on sintered pellets by the standard DC four terminal method between room temperature and 930 °C under air, using heating and cooling rates of 2–3 °C min^{-1}. Gold paste (T10112, Metalor Technologies Ltd., UK) was applied for both current and potential probes. A current of 100 mA (Keithley model 220, USA) was applied in both directions and resistance was calculated as a gradient of potential *vs*. current. This was converted to conductivity using the geometrical factor of the sample. To study an effect of oxygen partial pressure (aO_2) on conductivity, the electrical measurements were carried out at a constant temperature (800 °C) in non-humidified argon atmosphere. Oxygen partial pressure in the chamber was monitored with ZrO_2 oxygen sensor.

Thermogravimetric analysis (TGA) was used to monitor an amount of oxygen sorbed/desorbed by the perovskites and to evaluate the total oxygen content in the LNF sample. Measurements were carried out with a NETZSCH TG 209 instrument (NETZSCH-Geraetebau GmbH, Selb, Germany) on powders under air, argon and H_2–Ar (5% H_2–95% Ar) in a temperature range of 20–905 °C at a heating/cooling rate of 5 °C min^{-1}. An initial weigh of samples was about 60 mg. The effect of buoyancy was corrected in special runs with an alumina crucible under corresponding gas atmospheres.

3. Results and discussion

3.1. Phase composition and crystal structure at room temperature

3.1.1. Phase composition, crystal structure and thermochemical stability of LNF in air and in argon atmosphere

According to XRD and NPD recorded at room temperature, A-site deficient LNF has rhombohedral symmetry, space group $R\bar{3}c$ (No. 167). LNF has parameters $a = 5.5076(4)$ Å and $c = 13.2600(9)$ Å. Two very weak diffraction peaks corresponding to NiO were found in the XRD pattern of the LNF composition recorded in the reflection mode before and after calcination at 1350 °C. Refinement of the neutron powder diffraction pattern, which contains six clearly distinguished diffraction peaks of NiO, showed that LNF contains 5.2 mol% NiO with parameters $a = 2.9542(2)$ Å and $c = 7.2275(10)$ Å (space group $R\bar{3}m$, No. 166) as a secondary phase. It could indicate that there is no A-site deficiency in these perovskites. The initial material $La_{0.95}Ni_{0.6}Fe_{0.4}O_{3-\delta}$ can be better represented as a mixture of stoichiometrical phase $LaNi_{0.58}Fe_{0.42}O_{3-\delta}$ and NiO (Table 1).

Oxygen content in LNF was calculated assuming that both Ni and Fe cations have oxidation state 3+ (Table 1). In addition, oxygen content per formula unit ($3 \pm \delta$), can be measured by TGA from the weight loss of a sample during its decomposition in H_2–Ar atmosphere (Table 1). The value of oxygen content measured by TGA is lower than the calculated one. Oxygen content was, then, recalculated for the mixture of $LaNi_{0.58}Fe_{0.42}O_{3-\delta}$ and NiO. The recalculated value is low and comparable with the measured by TGA (Table 1).

According to TGA, LNF has good thermochemical stability in air and in argon during thermal cycling (TC) up to 800 °C. However, slight reversible weight loss (up to 0.13 ± 0.02 wt.%) was revealed in argon atmosphere at a temperature higher than 800 °C. XRD analysis did not show any difference between LNF powder before and after TC in non-humidified argon atmosphere. NPD analysis was, then, carried out for LNF-red, which was reduced under argon ($p(O_2) \sim 10^{-3}$ bar) for 12 h at 800 °C. LNF-red has also rhombohedral symmetry, space group $R\bar{3}c$ and contains 7.1 mol% NiO as a secondary phase. In this case, the lattice parameters are slightly higher for both perovskite constituent ($a = 5.5127(3)$ Å and $c = 13.2755(1)$ Å) and NiO ($a = 2.9566(2)$ Å and $c = 7.2344(9)$ Å). NiO content in LNF-red is higher than a nominal A-site deficiency in LNF, indicating partial decomposition. However, La_2O_3 or related phases were not observed in the NPD pattern of LNF-red, which could be due to the detection limit of NPD.

3.1.2. Phase composition of modified lanthanum iron nickelates in air

Phase composition of modified LNF varies depending on type and amount of oxide additives (Fig. 1 and Table 2). Formation of solid solutions was observed in the case of the addition of 2 mol% MnO_2, 2 mol% TiO_2, 2 mol% LSM and 10 mol% LSM (Fig. 1). It seems to be reasonable if we compare the ionic radii of Mn, Ti, Ni and Fe cations in high oxidation state: $r^{(VI)}_{Mn^{3+}} = 0.65$ Å, $r^{(VI)}_{Ti^{3+}} = 0.67$ Å, $r^{(VI)}_{Ni^{3+}} = 0.60$ Å and $r^{(VI)}_{Fe^{3+}} = 0.645$ Å [16]. A surprising result was noticed for LNFM2 and LNFT2. NiO as a secondary phase was present in both LNFM2 and LNFT2 compositions (and not MnO_2 and TiO_2 or related oxides). NPD measurement was carried for LNFM2.

Table 1
Oxygen content in LNF.

Abbreviation	Composition	Oxygen content theoretical	[a]Oxygen content at 800 °C	Representation of the composition as two-phase mixture	[b]Recalculated oxygen content for the mixture
LNF	$La^{3+}_{0.95}Ni^{3+}_{0.6}Fe^{3+}_{0.4}O_{3-\delta}$	2.925	2.872 ± 0.005	$La^{3+}Ni^{3+}_{0.58}Fe^{3+}_{0.42}O_{3-\delta}$ + 5.2 mol% NiO	2.896

[a] The oxygen content was determined from weight change of LNF during its reduction in non-humidified H_2–Ar.
[b] Theoretical oxygen content recalculated for two-phase mixture.

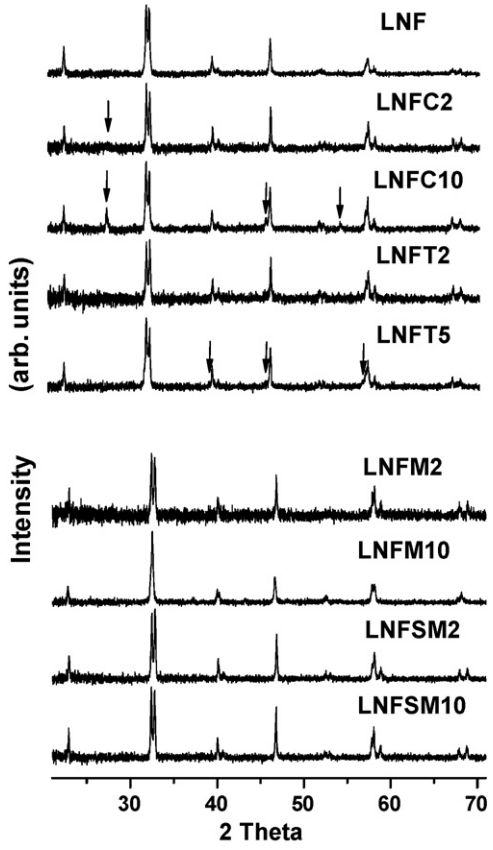

Fig. 1. XRD patterns of the modified compositions in air at room temperature.

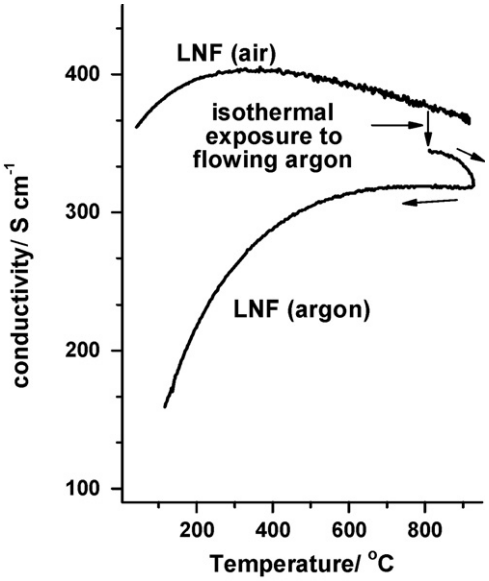

Fig. 2. Electronic conductivity of LNF in air and argon. Electronic conductivity measured in argon atmosphere is presented for heating up (800–900 °C) and cooling down (100–900 °C) stages, which is marked on diagram by arrows.

Refinement of the NPD pattern of LNFM2 also showed the presence of 6.8 mol% NiO, which is very close to the nominal A-site deficiency in LNFM2 (7 mol%, Table 2). It could indicate that the main fraction of manganese oxide substitutes for Ni in the B sublattice. Ni cations are displaced from the perovskite structure and segregate as a secondary phase, further increasing concentration of NiO. Similar to the parent LNF, LNFM2 composition can be represented as a mixture of a stoichiometrical phase $LaNi_{0.56}Fe_{0.42}Mn_{0.02}O_{3-\delta}$, which contains Ni, Fe and Mn on the B sublattice, and NiO as a secondary phase. $LaNi_{0.56}Fe_{0.42}Mn_{0.02}O_{3-\delta}$ has rhombohedral structure (space group $R\bar{3}c$, No. 167) with larger parameters ($a = 5.5115(5)$ Å and $c = 13.2759(1)$ Å) compared to LNF. The displacement of Ni cations from the perovskite structure can take place in the case of TiO_2 additive (for LNFT2 and LNFT5). However, neutron powder diffraction measurements should be carried out to clarify the mechanism in more detail. In the case of LNFT5, a formation of a new phase containing La–Ti–O was revealed in addition to the perovskite constituent with rhombohedral structure (Fig. 1). CeO_2 has low solubility limit in perovskite structure, despite the ionic radius of cerium cations varies essentially depending on local environment: $r^{(XII)}_{Ce^{3+}} = 1.29$ Å, $r^{(VI)}_{Ce^{4+}} = 0.80$ Å [16]. Both LNFC2 and LNFC10 compositions contain slightly reduced ceria (Ce_6O_{11}) (Fig. 1). In the case of LNFM10, a phase transformation to lower symmetry was observed.

3.2. Electrical conductivity of LNF in air and argon

Fig. 2 illustrates temperature dependences of electrical conductivity of LNF in air. LNF exhibits semiconducting conductivity under air in a temperature range of 25–300 °C, which is in accordance with the previous results [1,4]. Activation energy (E_a) evaluated for this temperature range amounts to 0.04 eV (Table 2). Conductivity of LNF decreases with further increase in temperature, indicating metallic-like behaviour. LNF sample was, then, exposed to argon atmosphere at 800 °C and temperature dependence of conductivity was, further, measured (Fig. 2). The total value of conductivity decreases by about 25% under argon atmosphere (from 400 S cm^{-1} to 304 S cm^{-1} at 500 °C). In addition, small hysteresis was observed at high temperatures. Conductivity of LNF decreases during heating up stage in a temperature range of 800–900 °C, indicating metallic-like behaviour. Electronic conductivity of LNF was almost constant during the cooling down stage between 700 °C and 900 °C. Only semiconducting conductivity was observed further during cooling down to room temperature (Fig. 2). Activation energy, which was evaluated for a temperature range of 100–700 °C, increases up to

Table 2
Phase composition and activation energy of conductivity (for regions with semiconducting type of conductivity).

Sample	Nominal A-site deficiency	Phase composition		E_a (eV)	
		Perovskite constituent	Additional phases	In air	Under argon
LNF	5	LNF	NiO	0.04 ± 0.001 (50–300 °C)	0.09 ± 0.001 (100–700 °C)
LNFC2	7	LNF	NiO, CeO_{2-x}	0.05 ± 0.001 (50–300 °C)	0.09 ± 0.01 (100–930 °C)
LNFC10	15	LNF	NiO, CeO_{2-x}	0.05 ± 0.001 (50–350 °C)	0.12 ± 0.01 (100–930 °C)
LNFT2	7	LNFT	NiO	–	–
LNFT5	10	LNFT	NiO, La–Ti–O phase	0.06 ± 0.003 (50–550 °C)	–
LNFM2	7	LNFM	NiO	0.04 ± 0.003 (50–300 °C)	0.10 ± 0.01 (100–680 °C)
LNFM10	14.5	LNFM	NiO	0.10 ± 0.01 (50–900 °C)	0.16 ± 0.02 (100–900 °C)
LNFSM2	4.9	LNFSM	NiO	0.04 ± 0.002 (50–300 °C)	0.11 ± 0.01 (100–900 °C)
LNFSM10	4.5	LNFSM	NiO	0.07 ± 0.002 (50–635 °C)	0.12 ± 0.01 (100–900 °C)

0.09 eV. The lower activation energy predicts that small polaron conduction dominates.

Transport of small polarons in an ionic solid can be described by either a small polaron band mechanism or small polaron hopping mechanism. The electronic conductivity (σ_e) is proportional to the number of charge carries (n), their charge (e) and mobility (μ):

$$\sigma_e = ne\mu \quad (1)$$

Therefore, the value of mobility can be evaluated for the parent LNF with rhombohedral structure with the unit cell volume $V_{rhomb} = 0.866a^2c$, where a and c are the lattice parameters. The numbers of carriers was obtained assuming that one electron per Ni cation is involved in the charge transfer process, the rhombohedral unit cell volume contains six formula units and Ni occupancy onto the B sites amounts to 60 mol%: $n = (1 \times 6 \times 0.6)/(0.866a^2c)$. It was found that $\mu \sim 0.24\ cm^2\ s^{-1}\ V^{-1}$ at 500 °C. This value is higher than the limiting value ($\sim 0.1\ cm^2\ s^{-1}\ V^{-1}$) usually taken as the minimum value for band conduction [17]. The conduction band in LNF can be formed by direct overlapping of 3d Ni–3d Ni and 3d Ni–2p O orbitals. Both types of hybridization, 3d Ni–3d Ni or 3d Ni–2p O, depend on the O–Ni bond length in the crystal structure. 3d Fe orbitals could also contribute to the band formation. However, for substituted $LaNiO_3$ ($LaFe_{1-x}Ni_xO_{3-\delta}$ and $La_{0.9}Sr_{0.1}Ga_{1-x}Ni_xO_{3-\delta}$) was noticed that metallic-like conductivity was observed in the case of high Ni occupancy of the B sublattice (more than 50 mol%) [2,3,8]. Probably, the continuousness of the 3d Ni–3d Ni hybridization through the crystal structure can, in addition, vary depending on the number of Ni neighbours in the second coordination shell. Since NPD analysis showed that the reduced LNF (LNF-red) has larger lattice parameters compared to the parent LNF it is reasonable to expect the decrease in the 3d Ni–2p O and 3d Ni–3d Ni hybridizations and, as a consequence, the decrease in the width of the Ni/Ni–O hybrid band. However, an effect of temperature on the change of conductivity from semiconducting to metallic-like has not been fully understood yet. Most likely, micro-mechanism of band formation and variation of its components with temperature are of great importance: whether the width of the Ni/Ni–O hybrid band is determined by the intensity of super-exchange interactions via the oxygen (3d Ni–2p O–3d Ni) or direct overlap of 3d Ni–3d Ni orbitals or both.

3.3. Electrical conductivity of modified lanthanum iron nickelates

Figs. 3–5 illustrate transport characteristics of the modified LNF compositions in air and under argon atmosphere. Activation energy evaluated for the regions with semiconducting conductivity is listed in Table 2. LNFC2, LNFM2 and LNFSM2 exhibit similar trends in the change of electronic conductivity as the parent LNF (Fig. 3). The change from semiconducting to metallic-like conductivity was observed at 300 °C. The activation energy evaluated for LNFC2, LNFM2 and LNFSM2 amounts to 0.04–0.05 eV (Table 2). However, the absolute value of the electronic conductivity varies slightly. The electronic conductivity of LNFC2, LNFSM2 and LNF is comparable, whereas that of LNFM2 is slightly lower. Since the lattice parameters of LNFM2 are slightly larger compared to LNF, the overlapping of 3d(Ni)–3d(Ni) or 3d(Ni)–2p(O) orbitals could be less, leading to the formation of a narrower conduction band.

The presence of a secondary phase could also affect the electronic conductivity of modified LNF compositions. LNFM2 contains about 7 mol% NiO. It is known, that NiO is a p-type semiconductor and its resistivity strongly depends upon the concentration of cation vacancies [18]; however, as only 7% is present it will have little effect other than dilution upon conductivity. The total electronic conductivity could essentially drop at a higher concentration of NiO secondary phase, as it may be in the case of LNFM10. It should be mention that the change in the symmetry of the perovskite constituent in the LNFM10 is an important factor, also affecting the total electronic conductivity. The influence of the secondary phase on the electronic conductivity can be also demonstrated by the example of the LNF modified by CeO_2. The electronic conductivity of LNFC10 drops by about a factor of 1.5 compared to LNF and LNFC2 (Fig. 3). Ceria is known as a fast ionic conductor. Oxygen vacancies and electrons are the main charge carriers. LNF is a p-type conductor (Fig. 4), with much higher total conductivity compared to ceria [1,3,4,19,20]. Most probably, the total conductivity of LNFC10 composition will be determined by CeO_{2-x} distribution through the volume of the material where it blocks conduction pathways between LNF grains. The electronic conductivity of LNFT5 is lower by about a factor of 2 compared to the parent LNF. This could be caused by three different effects: (i) the presence of La–Ti–O containing phase, (ii) incorporation of Ti into the B sublattice, forming perovskite structure containing Ni, Fe and Ti onto the B sublattice and (iii) increase in NiO secondary phase concentration due to displacement from the

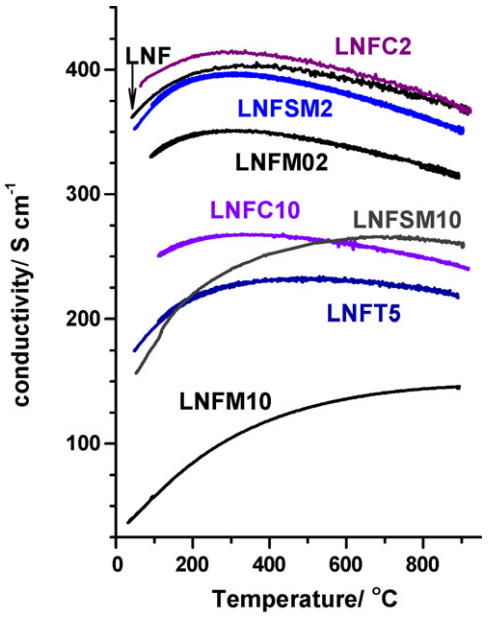

Fig. 3. Temperature dependence of electronic conductivity of the modified compositions, $p(O_2) = 0.21$ atm.

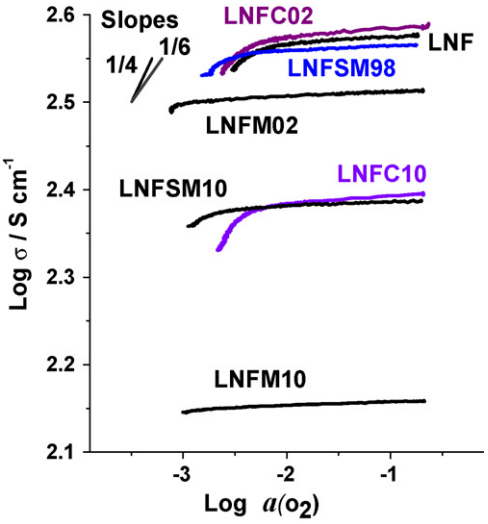

Fig. 4. Conductivity of the modified compositions during isothermal exposure under argon atmosphere; 800 °C.

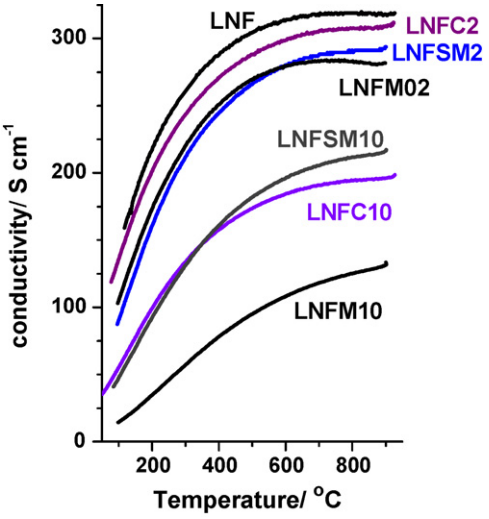

Fig. 5. Temperature dependence of electrical conductivity of the modified compositions under argon atmosphere; data are presented for the cooling down stage.

perovskite structure. In the case of LNFT5, a shift of the temperature of the semiconducting-metallic transition to 550 °C was observed (Fig. 3) possibly indicating a change in electronic properties of the LNF due to Ti substitution. LNFSM10 with the same structure as the parent LNF (Fig. 1 and Table 2) exhibits lower electronic conductivity and metallic-like conductivity at high temperatures (between 600 °C and 900 °C).

Fig. 4 illustrates the effect of oxygen partial pressure on the conductivity of the modified LNF compositions at 800 °C in the coordinates $\log\sigma$ *vs.* $\log a_{(O_2)}$. The measurements were carried out in a narrow oxygen partial pressure range ($0.21 \leq a_{O_2} \leq 1 \times 10^{-3}$) because these compositions are not stable under strong reducing conditions. The total conductivity of LNFC2, LNFC10, LNFM2, LNFM10, LNFSM2 and LNFSM10 decreases with the lowering of oxygen partial pressure, indicating these compositions are p-type conductors. Further, the temperature dependence of conductivity was measured under argon atmosphere (Fig. 5, cooling down stage). Similar to LNF, the electronic conductivity of LNFM2 was almost constant in a temperature range of 680–900 °C, whereas all other compositions showed semiconducting conductivity in the whole temperature range investigated (Fig. 5). Notice that LNFM10 initially in air showed semiconducting behaviour in a wide temperature range (Fig. 3). Activation energy increased by about a factor of 2–3, but it still did not exceed 0.16 eV (the highest value of E_a was observed for LNFM10) (Table 2). Since similar semiconducting behaviour was observed in a wide temperature range for LNF itself and for the modified LNF with different phase compositions (Fig. 1 and Table 2), one can assume that processes taking place in the structure of the perovskite constituent are responsible for the change in the value and type of conductivity (Fig. 5). Probably, under argon atmosphere a fraction of Ni^{2+} cations on the B sublattice of perovskite constituent increases as compared to oxidizing conditions. The Ni^{2+} d-electrons are localized. This could dramatically change degree of 3d Ni–2p O and 3d Ni–3d Ni hybridization, its continuousness through the perovskite structure and, finally, prevent small-polaron band conduction.

4. Conclusions

Phase composition, structure and electronic conductivity of $La_{0.95}Ni_{0.6}Fe_{0.4}O_{3-\delta}$ itself and modified by small additives (up to 10 mol%) of MnO_2, TiO_2, CeO_2, and Sr-containing manganese perovskite were investigated in air and after reduction in argon atmosphere. A-site deficient LNF can be represented as a mixture of stoichiometrical phase $LaNi_{0.58}Fe_{0.42}O_{3-\delta}$ with rhombohedral structure and NiO as a secondary phase. Concentration of secondary phase increases after reduction under argon atmosphere. Phase composition of the modified LNF varies depending on type and amount of oxide additive. One can distinguish the following situations: coexistence of LNF and the added oxide; added oxide and LNF interacts with a formation of a new phase; a structural transformation of modified LNF; and formation of solid solutions with the same structure as the parent LNF. In the case of modification by small amount of MnO_2, manganese cations seem to incorporate into the perovskite structure and displace nickel cations. The last segregates as an individual phase, increasing the concentration of NiO secondary phase. A similar process was assumed to take place in the case of modification by TiO_2. Despite the difference in phase composition, a low level of doping does not change value of conductivity and temperature of the semiconducting-metallic transition (~300 °C) of the modified LNF compositions. Modification with 5 mol% oxide additive or higher, in general, leads to a decrease in the electronic conductivity and the extension of the region with the semiconducting conductivity (up to about 600 °C). Under argon atmosphere LNF and modified compositions containing different amount of oxide additives show semiconducting behaviour in a wider temperature range. The factors governing the semiconducting-metallic transitions have been not fully understood yet. It is necessary to take into account many types of interactions: the lattice structure and its disorder, the lattice behaviour giving rise to small polaron formation and moving as well as the band structure (including its continuousness through the crystal lattice and ratio of Ni^{2+}/Ni^{3+} cations). All these effects take place simultaneously and can interfere or complement each other in different ways with the temperature variation.

Acknowledgements

The authors gratefully acknowledge Dr. E. Suard and Mr. L. Gendrin (ILL Grenoble) for help with neutron diffraction measurements and EPSRC for financial support. One of authors (EK) acknowledges to Royal Society of London for the travel grant to the conference "Fuel Cell Science and Technology 2008".

References

[1] R. Chiba, F. Yoshimura, Y. Sakurai, Solid State Ionics 124 (1999) 281–288.
[2] K. Świerczek, J. Marzec, D. Pałubiak, W. Zając, J. Molenda, Solid State Ionics 177 (2006) 1811–1817.
[3] E. Konysheva, J.T.S. Irvine, J. Mater. Chem. 18 (2008) 5147–5154.
[4] J. Knudsen, P.B. Friehling, N. Bonanos, Solid State Ionics 176 (2005) 1563–1569.
[5] P.A. Cox, Transition Metal Oxides, Clarendon Press, Oxford, 1995, p. 283.
[6] S.P. Jiang, Y. Zhen, Solid State Ionics 179 (2008) 1459–1464.
[7] E. Konysheva, H. Penkalla, E. Wessel, J. Mertens, U. Seeling, L. Singheiser, K. Hilpert, J. Electrochem. Soc. 153 (2006) A765–773.
[8] N.J. Long, F. Lecarpentier, H.L. Tuller, Electroceramics 3 (1999) 399–407.
[9] W.J. Quadakkers, J. Piron-Abellan, V. Shemet, L. Singheiser, Mater. High Temp. 20 (2003) 115–127.
[10] E. Konysheva, U. Seeling, A. Besmehn, L. Singheiser, K. Hilpert, J. Mater. Sci. 42 (2007) 5778–5784.
[11] H.U. Anderson, F. Tietz, in: S.C. Singhal, K. Kendall (Eds.), High Temperature Solid Oxide Fuel Cells: Fundamentals, Design and Applications, Elsevier Advanced Technology, 2003, pp. 173–195.
[12] E. Konysheva, J. Laatsch, E. Wessel, F. Tietz, N. Christiansen, L. Singheiser, K. Hilpert, Solid State Ionics 177 (2006) 923–930.
[13] H.M. Rietveld, Acta Crystallogr. 22 (1967) 151–152.
[14] H.M. Rietveld, J. Appl. Crystallogr. 2 (1969) 65–71.
[15] J. Rodriguez-Carvajal, Physica B 192 (1993) 55–69.
[16] R.D. Shannon, C.T. Rewitt, Acta Crystallogr. B 25 (1969) 925–946.
[17] A.J. Bosman, H.J. val Daal, Adv. Phys. 19 (1970), p. 1.
[18] M.A. Wittenhauer, L.L. Van Zandt, Phil. Mag. B 46 (1982) 659–663.
[19] P. Kofstad, Nonstoichiometry, Diffusion and Electrical Conductivity in Binary Metal Oxides, John Wiley & Sons Inc., New York, 1972, p. 276.
[20] H.L. Tuller, A.S. Nowick, J. Electrochem. Soc. 126 (1979) 209–217.